

## Numerical Simulation of Temperature Logs in High Temperature Wells: Towards the Application to the RN-15/IDDP2 Well

Jia Wang\*, Fabian Nitschke, Emmanuel Gaucher and Thomas Kohl

Adenauerring 20b, Building 50.40, 76131 Karlsruhe, Germany

\*jia.wang@kit.edu

**Keywords:** IDDP-2, DEEPEGS, Numerical simulation, Formation temperature, Fluid loss.

### ABSTRACT

In the frame of the EU Horizon 2020 DEEPEGS project and the IDDP2 project, the well RN-15 located in the Reykjanes geothermal field (Iceland) was deepened. So far, this well, namely RN-15/IDDP-2 is the deepest geothermal well drilled in Iceland with a final depth of 4,659 m, a measured bottom-hole temperature of 427°C and a fluid pressure of 34 MPa. During drilling, several temperature logs were run whilst water was injected continuously to cool down the equipment in the borehole due to the high-temperature environment. The objective of our work, as part of the DEEPEGS project, is to apply numerical simulation methods to estimate the formation temperature and fluid loss along the well path, based on the recorded temperature logs acquired under dynamic conditions, during and after drilling. This is of particular interest for the development and understanding of the deep geothermal reservoir.

Our approach comprises the development of a transient thermal model in which the temperature evolution of the well and the surrounding formation is simulated. The numerical tool enables the use of the whole history of fluid circulation data. In this work, we first simulated synthetic models in order to investigate the feasibility of (1) using temperature logs obtained under borehole cooling conditions to estimate the static formation temperature (SFT) and (2) characterizing fluid losses from temperature logs. The results showed that applying simple temperature correction methods on the non-shut-in temperature data could lead to large errors for SFT estimation even at low flow rates. Fluid loss leads to a local gradient increase in the vertical temperature profile. The magnitude of the gradient change depends both on the percentage of fluid loss and the flow rate. However, for fluid losses below 30% or relatively high flow rates 20-50 L/s (velocities 0.5~1.3 m/s), the temperature gradient increase is independent of the flow rate. The knowledge and experience gained from the synthetic models provide insights for future work when the real temperature logging data are used to constrain the far-field formation temperature and to estimate the fluid loss. Herein, we also present some first results on the temperature analysis in the RN-15/IDDP2 well using real long-term drilling and logging data.

### 1. INTRODUCTION

The RN-15/IDDP2 deep geothermal well of the DEEPEGS EU project at Reykjanes, Iceland represents the hottest geothermal well ever drilled with fluids at supercritical conditions at the bottom-hole (426°C, 340 bar) (Friðleifsson et al., 2017). The drilling operation of RN-15/IDDP2 began with the deepening of the 2.5 km deep RN-15 well. The drilling took 168 days and was completed on the 25th of January at a 4,659 m depth. A complete loss of circulation fluid occurred below 3,200 m. During the drilling, several temperature logs were recorded with water being injected continuously to cool down the equipment in the borehole due to the high-temperature environment. These temperature logs will be analyzed for two major purposes: one is to estimate the static formation temperature (SFT), the other one is to characterize the fluid loss.

Estimation of the SFT is usually done by measuring the bottom-hole temperature (BHT) when the drilling circulation has stopped and the borehole fluid temperature gradually recovers to the unperturbed formation temperature. However, the measured BHT is usually lower than the true SFT due to the thermal disturbances of the drilling mud and, therefore, needs to be corrected (Deming, 1989; Goutorbe et al., 2007). Various temperature correction methods based on different simplified physical models have been developed, e.g., the Horner-plot method (or constant line source method (Bullard, 1947; Dowdle & Cobb, 1975)); the spherical and radial heat flow method (Ascencio et al., 1994, 2006); the Hasan-Kabir method (Hasan & Kabir, 1994) and the Kutasov-Eppelbaum method (Kutasov & Eppelbaum, 2005). These methods rely on linear or non-linear regression models that describe the relationship between measured BHT and time functions accounting for the transient effects of thermal recovery during effects during the shut-in phase of the borehole (Verma et al., 2006a,b; Wong-Loya et al., 2012).

Examples of using temperature measurements in boreholes to identify fluid loss or feed zones from temperature data are also found in many earlier studies. For example, Pehme et al. (2010) identified hydraulically active fractures in dolomite and sandstone aquifers; Klepikova et al. (2011) estimated local transmissivities and hydraulic head differences; Nian et al. (2015) predicted flow rates in oil and gas production wells. These authors emphasized the satisfactory accuracy of temperature-derived flow velocities compared to direct flow measurement.

In this paper, the numerical approach to simulate temperature logs in the high-temperature environment using our in-house numerical simulation tool is introduced. Synthetic data that reflect possible logging conditions such as permanent cooling or fluid loss zones in the RN-15/IDDP2 well is assumed. We first provide an example of estimating SFT in an extremely high-temperature well, which is continuously cooled down during logging. The impact of using non-shut-in temperature logs for the SFT estimation is examined. Moreover, we investigate how temperature logs can be used for characterizing fluid loss in the borehole. In the end, some first results of using real drilling data to evaluate long-term temperature perturbations in the well are also presented.

## 2. METHODS

### 2.1 Numerical Methods

In this study, the thermal behavior of the wellbore and its surrounding formation is modeled using an in-house numerical simulation tool. The simulator is an application developed based on the MOOSE framework (Gaston et al., 2009) which consists of different physics modules that can be fully coupled for solving variables in an implicit manner.

Figure 1 shows the scheme of the wellbore heat transfer model considered in this work. Different wellbore regions such as the wellbore fluid (Region 1), drill pipe (Region 2), annulus (Region 3), casings and formation (Region 4) were considered. The simulator assumes the wellbore to be treated either as a 1-D or 2-D structure depending on the complexity of the studied problem. For example, the well can be simplified as having 1-D flow embedded in the 2-D formation (Figure 1a) or the 2-D wellbore completions can be explicitly considered in the model (Figure 1b). Temperatures in the four regions are solved as individual variables ( $T_1$ ,  $T_2$ ,  $T_3$ , and  $T_4$ ). These variables are linked through the interfacial heat transfer relationships between the fluid and solid. The injection fluid was assumed to be pure liquid water. Fluid properties such as density, viscosity, and heat capacity were calculated according to the IAPWS-IF97 formulation. In our models, we assumed cylindrical geometries, incompressible fluid, axial-direction flow, an impermeable rock formation, no temperature gradient in the radial direction within the fluid, negligible thermal dissipation and expansion effects.

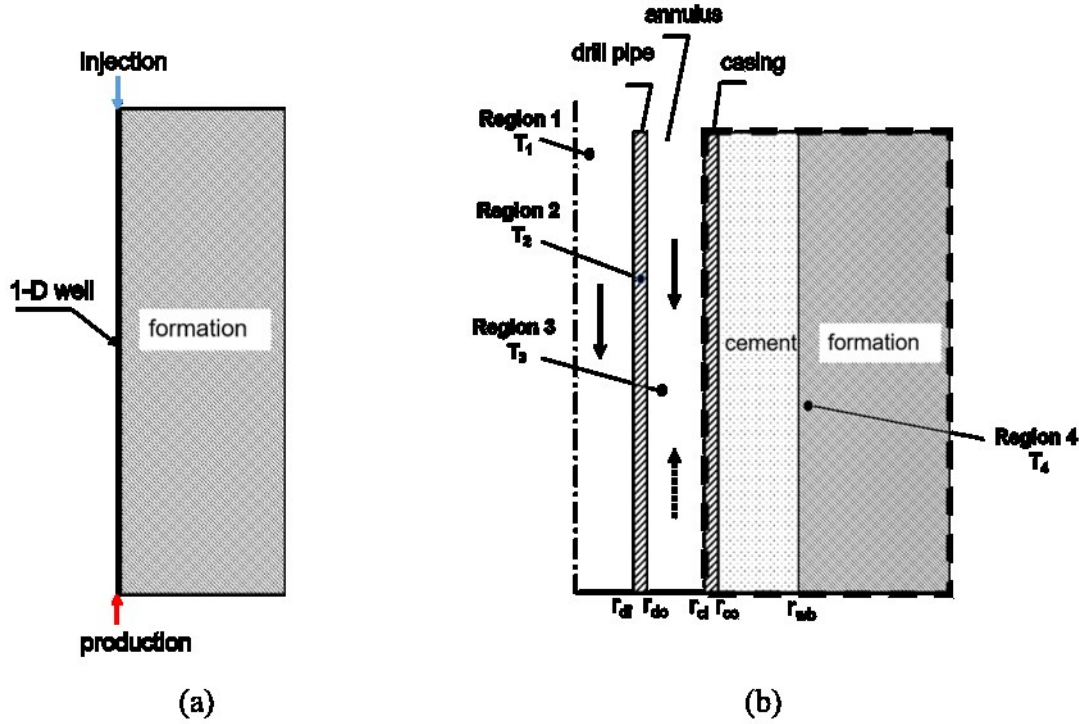


**Figure 1: Scheme of the heat exchange model between the wellbore and the formation. (a) Simplified 1-D well model; a straight, non-cased 1-D well is embedded in the two-dimensional formation. The fluid is injected at the wellhead or produced at the well-bottom. (b) 2-D well complex model; governing equations are solved in four regions- the fluid inside the drill pipe (Region 1), the drill pipe wall (Region 2), the annulus (Region 3), the casing-cement-formation (Region 4). The solid arrow pointing downwards and the dashed arrow pointing upwards in the annulus refer to coflow (injection) and counterflow (production) scenarios in the wellbore, respectively.**

The governing equations for the drilling pipe fluid (Region 1) and annulus fluid (Region 3) are:

$$\frac{\partial v_z}{\partial z} = 0, \quad (1)$$

$$\rho C_p \left( \frac{\partial T}{\partial t} + v_z \frac{\partial T}{\partial z} \right) - \frac{\lambda}{r} \frac{\partial T}{\partial r} - \lambda \frac{\partial^2 T}{\partial^2 r} - \lambda \frac{\partial^2 T}{\partial^2 z} = 0 \quad (2)$$

where  $\rho$ ,  $C_p$ ,  $\lambda$  are the density, heat capacity and thermal conductivity.  $v_z$  is the axial fluid velocity.

The governing equations for the drilling pipe (Region 2), casings and formation (Region 4) are:

$$\rho C_p \frac{\partial T}{\partial t} - \frac{\lambda}{r} \frac{\partial T}{\partial r} - \lambda \frac{\partial^2 T}{\partial^2 r} - \lambda \frac{\partial^2 T}{\partial^2 z} = 0 \quad (3)$$

The boundary and initial conditions are given in Table 1.

## 2.2 SFT Estimation

The Horner-plot method (HM) was chosen to estimate SFT due to its great simplicity and wide application. This method assumes the thermal effect of drilling as a constant linear heat source. The mathematical form of the HM is given by:

$$T_s = T_i + \frac{q}{4\pi\lambda_s} \ln \frac{t_c + t_s}{t_s}, \quad (4)$$

where  $T_s$  is the shut-in temperature,  $T_i$  is the SFT,  $t_s$  and  $t_c$  are the shut-in time and circulation time respectively,  $q$  is the heat extraction rate. SFT can be obtained when  $t_s$  approaches  $\infty$ .

**Table 1: Boundary and initial conditions for the wellbore thermal model. After Wang et al. (submitted).**

BC & IC	Expression	Description
IC	$T_i(r, z, t = 0) = T_f(r, z), i = 1, 2, 3, 4 \quad \forall r$ $, 0 \leq z \leq H$	The initial temperature is equal to the formation temperature
BC1	$v_{z_i} = \frac{\dot{V}_i}{\rho A_i}, z = 0, i = 1, 3$	The velocity of the drilling pipe fluid and the annulus fluid are calculated according to the mass flow rate at the wellhead
BC2	$q = -\lambda \left( \frac{\partial T}{\partial r} \right) \Big _{\Gamma_{ij}} = h(T_i - T_j), \text{ on } \Gamma_{12}, \Gamma_{23}, \Gamma_{34}$	Heat flux across the solid-fluid interface is determined by the heat transfer coefficient times the temperature difference between fluid and solid wall
BC3	$-\lambda \left( \frac{\partial T_1}{\partial r} \right) = 0 \text{ at } z = H, z = 0$	No thermal gradient at the surface and bottom of the reservoir
BC4	$T_4(r = \infty, z, t) = T_f(r, z) \text{ at } r = \infty$	Formation temperature at the far-field remains undisturbed
BC5	$T_1(r, z = 0, t) = T_{inj} \text{ at } 0 < r < r_1, z = 0$	The temperature at the well-head equals the injection temperature
BC6	$T_1(z = H, t) = T_3(z = H, t)$	The fluid temperature of the drilling pipe fluid and the annulus fluid at the bottom hole are equal. This is only validated for the counterflow scenario (mud circulation)

$A_i$  is the flow cross-section,  $\Gamma_{ij}$  is the interfacial area between the fluid and solid structures, e.g., drilling pipe, casing and formation,  $z_{max}$  is the well depth,  $T_f(r, z)$  is the formation temperature,  $T_{inj}$  is the injection temperature of the fluid,  $h$  is the heat transfer coefficient.

## 3. SIMULATIONS AND RESULTS

The numerical study was applied to the RN-15/IDDP2-well in Reykjanes. First, we present synthetic models where two major concerns are addressed: (1) whether simple BHT correction methods are still applicable to temperature logs obtained under borehole cooling scenarios; (2) how can the fluid loss be characterized from well temperature logs. In the second part of the study, the long-term temperature analysis of the well using real drilling data is presented.

### 3.1 Synthetic Models

Herein, we focus on the high-temperature environment temperature log simulations. For this purpose, a 500°C temperature is assumed for the formation around the RN-15/IDDP2 well at a 4,589 m depth. To investigate the impact of different formation temperature profiles on the simulation results, two different SFT profiles were used (Figure 2). The wellbore layout included the drilling pipe, annulus and several casings (Table 2). The injection temperature of the fluid was assumed to be 7°C.

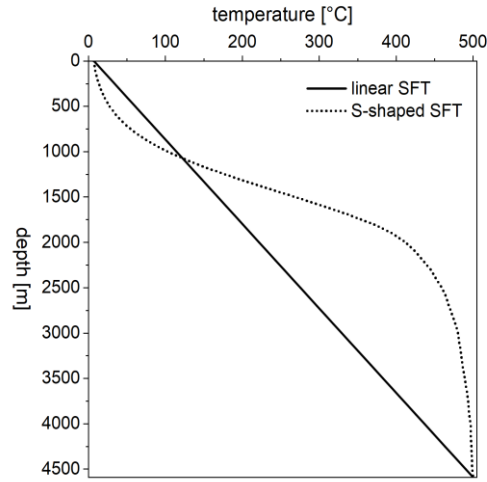


**Figure 2: Two different SFT profiles assumed in the high-temperature environment: linear SFT describes pure heat conduction in the formation, S-shaped SFT reflects typically occurring convection zones in the formation. After Wang et al. (submitted).**

**Table 2: Geometrical parameters of the wellbore**

	Inner radius (m)	Outer radius (m)	Cross-sectional area (m <sup>2</sup> )	Depth (m)
Drilling pipe	0.0352	0.0445	2.33x10 <sup>-03</sup>	0-4589
Casing i	0.0797	0.0889	4.87x10 <sup>-03</sup>	0-1304
Casing ii	0.11	0.122	8.75x10 <sup>-03</sup>	0-2941
Casing iii	0.1577	0.1699	1.26x10 <sup>-03</sup>	0-793
Annulus	0.0445	0.0797	1.37x10 <sup>-02</sup>	0-1304
	0.0445	0.11	3.18x10 <sup>-02</sup>	1304-4589

**3.1.1 SFT Estimation under Continuous Borehole Cooling**

The RN-15/IDDP2 well had been cooled continuously during and after the completion of the drilling, except for several short periods of warm-up. During these warm-up periods (five days), while injection in the drill string stopped, 4-5 L/s of fluid was still injected in the annulus to cool the casing and the logging tool. Before the warm-up, the well had been subjected to 10 days' cooling where 15 L/s was injected through the drill string and 45 L/s into the annulus. In our simulations studies of the synthetic scenarios, we varied the cooling flow rate in the annulus (0-5 L/s) and applied the HM to estimate the SFT using the temperature measurements inside the drilling pipe. The sensitivity of the SFT estimation result to the cooling flow rate in the annulus during the warm-up period was analyzed.

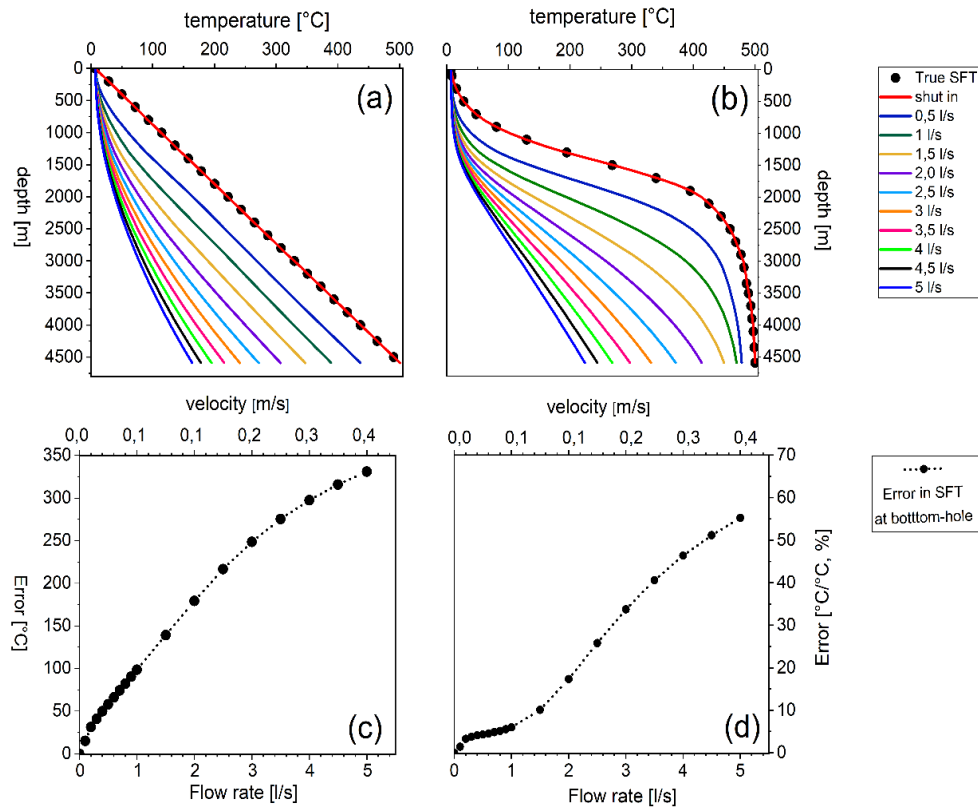


**Figure 3: Estimated SFT profile under different flow rates (0-5 L/s) in the annulus during the warm-up period versus depth when assuming (a) a linear SFT profile and (b) an S-shaped SFT profile (black dots represent the true SFTs, red lines represent the SFT estimates under real shut-in conditions). (c) Errors in the estimated SFT for the linear-shaped SFT profile case. (d) Errors in the estimated SFT for the S-shaped SFT profile case. After Wang et al. (submitted).**

The results of the SFT estimates under different cooling rates (Figure 3a,b) as well as the estimation error at the bottom-hole (Figure 3c,d) for the assumed two different SFT profiles are presented. As can be seen, the SFTs were all under-estimated using temperature measurements under borehole cooling conditions. Even under small flow rates under 0.7 L/s (the corresponding velocities  $\leq 0.05$  m/s), the estimation error at the bottom-hole was around 74°C and 24°C for the linear SFT and the S-shaped SFT scenario respectively. Moreover, the S-shaped SFT scenario tends to produce higher SFT estimation values than the linear SFT scenarios.

### 3.1.2 Fluid Loss Characterization

In this section, a series of temperature logs assuming different flow rates (dynamic conditions) and fluid losses are generated. These temperature logs were 'recorded' in the drilling pipe and then used as samples to characterize the fluid losses from different temperature responses. In our models, the fluid velocities in the annulus and the drill pipe were assumed equal, only the total amount of injected fluid was changed (5~50 L/s). The fluid was lost at a 3.35 km depth from the annulus due to the hydraulic connection to the formation and the percentage of fluid loss was varied (0~90%).

Figure 4 presents the simulated temperature logs under flow rates of 5L/s and 50 L/s for the S-shaped SFT profile. The results for the linear SFT profile were omitted since it was found that the temperature response to fluid loss was very similar for different SFT profiles. As expected, an increase in the local temperature gradient below the fluid loss zone for each of the temperature logs was observed. With a higher fluid loss, the temperature gradient gets deeper. The reason for such behavior is that the residence time of the fluid in the well becomes longer due to a higher fluid loss, which allows the fluid to gain more heat from the hotter surrounding. Further analysis of the temperature logs was done by computing the ratio of the temperature gradient below to above the feed point. Relationship curves between the temperature gradient ratio and the percentage of fluid loss under different flow rates are shown in Figure 5. It was found that when the fluid loss is relatively low ( $<30\%$ ), the gradient ratio tends to be independent of the flow rate. For fluid losses  $>30\%$ , the smallest temperature gradient ratios are observed for the lowest flow rate. Furthermore, the fluid loss seems to be independent of the flow rate when the flow rate is higher than 20 L/s.

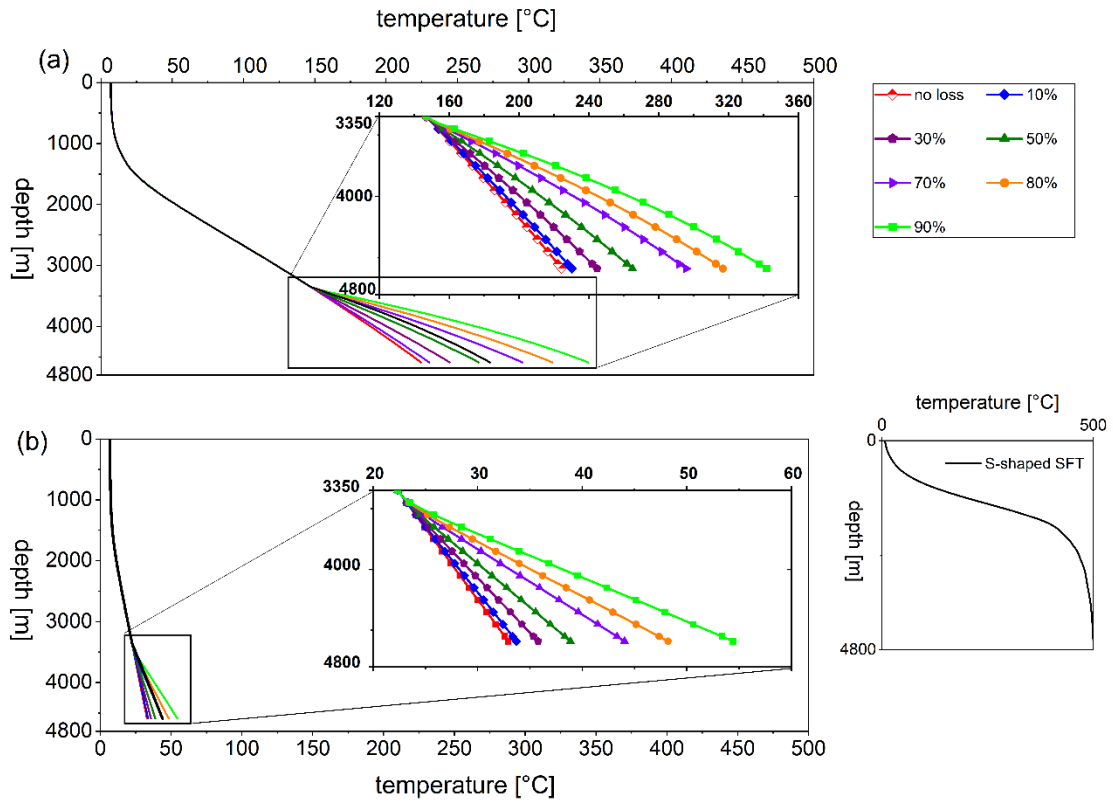


Figure 4: The simulated temperature logs under different fluid loss percentages assuming the S-shaped SFT profile. (a) Results for the 5L/s injection flow rate. (b) Results for the 50 L/s injection flow rate.

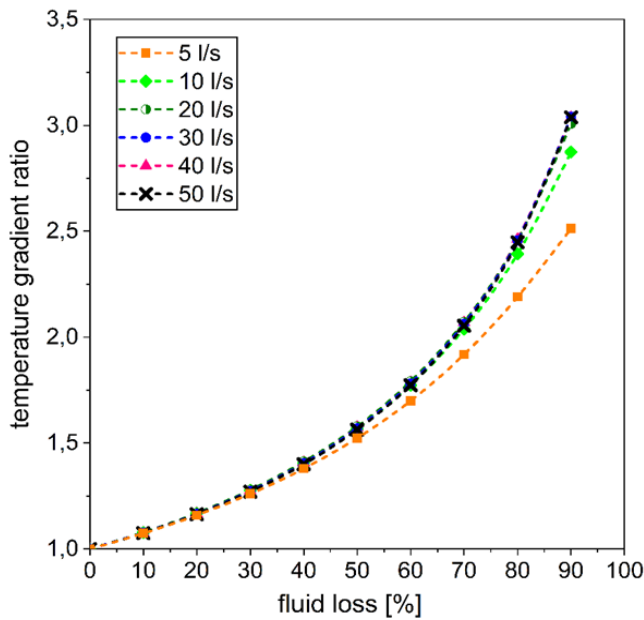


Figure 5: The ratio of temperature gradient below the fluid loss zone (3.5 km depth) to the gradient above the fluid loss zone versus the percentage of fluid loss (S-shaped SFT profile is assumed).

### 3.2 Real Data

As mentioned earlier, the principle goals of the numerical study are to estimate the SFT and the fluid loss along the well depth. To this end, real data such as the long-term injection rate, the recorded temperature logs, the logging speed need to be considered in the model. In this part, we present our first results on the application of drilling and logging data to the wellbore simulation.

#### 3.1.1 The Temperature Response in the Well to the Long-Term Variational Flow

The long-term temperature perturbation in the well due to drilling as well as its dynamic response to the flow rate variations is investigated.

To exclude the uncertainties from local variants such as the different cooling time due to the deepening of the well and the fluid loss, we only simulate the temperature change until 2.5 km depth. The injection flow rate curve for 145 days since the start of the deepening of the 2.5 km deep RN-15 well was applied in the simulation (Figure 6a).

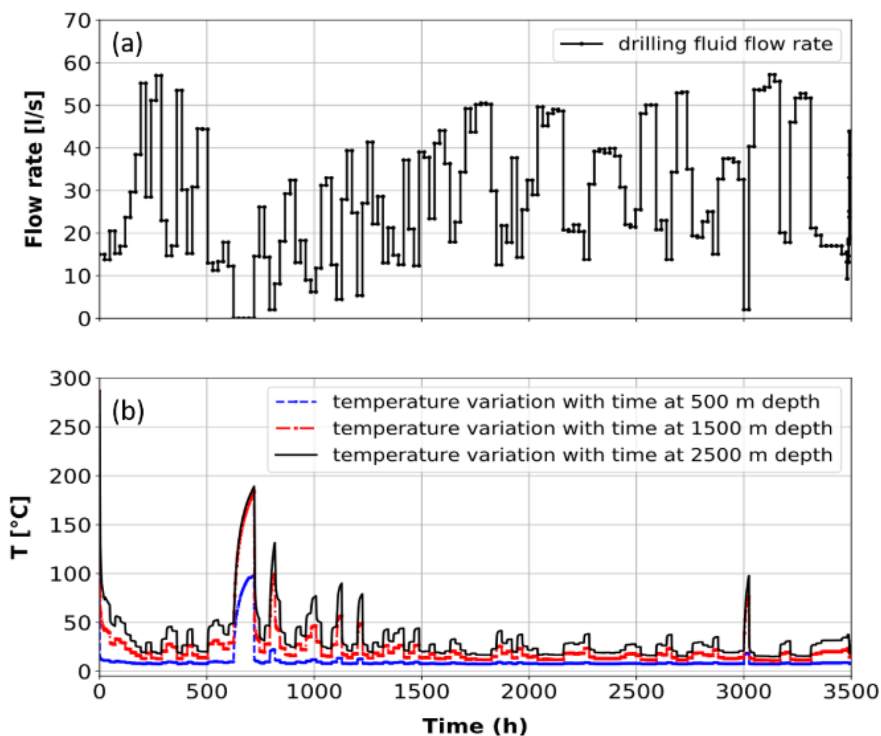


**Figure 6: Injection flow curve for 145 days since the start of the deepening of the RN-15 well (top); location temperature variation with time at different well depths (bottom).**

Figure 6a shows the temperature change with time at different well depths. The temperature response to the flow variation seems to be reasonable as the temperature perturbation is larger when the fluid rate increases. On the contrary, temperature perturbation is smaller when the fluid rate decreases.

### 3.1.2 The Primary Result on the SFT Estimation until 2.5 km

According to Friðleifsson et al. (2018), the steady-state temperature profile around the RN-15 well until 2.5 km has been studied and can be found in a database established by ISOR (the Iceland Geosurvey). We use the estimated SFT profile for the RN-15 well in this database as an initial approximation (Figure 7b). Several temperature logs that were conducted during the injection of cold fluid ( $\sim 7^{\circ}\text{C}$ - $8^{\circ}\text{C}$ ) were selected for numerical modeling. Here, we only present the simulation result for one dynamic temperature log which was surveyed after 145 days' injection. The tripping of the logging tool from the wellhead to 2.5 km lasted about 2 hours (Figure 7c) and the injected flow rate was increased during the logging (Figure 7a). The time step sizes during the simulation were adjusted according to the logging speed in order to have a depth-temporal match between the simulated and measured fluid temperature. The comparison between the simulation results and the measurements is shown in Figure 7d. It can be seen that the simulated temperatures are lower than the logged temperatures (maximum difference of  $3^{\circ}\text{C}$ ), which is also observed when comparing the simulation results and measurements for the other temperature logs. The reason for this might be due to an under-estimation in the SFT. In addition, the temperature gradient of the well fluid temperature in the first 500 m appears to be different from the measured one, which leads to a shift of the simulated temperature profile from the logged profile beneath. Therefore, the SFT profile above 500 m depth should be more carefully evaluated. Based on this primary result, the next step of our study is to invert the SFT around The RN-15/IDDP-2 well by using the SFT profile from the database as a first guess.

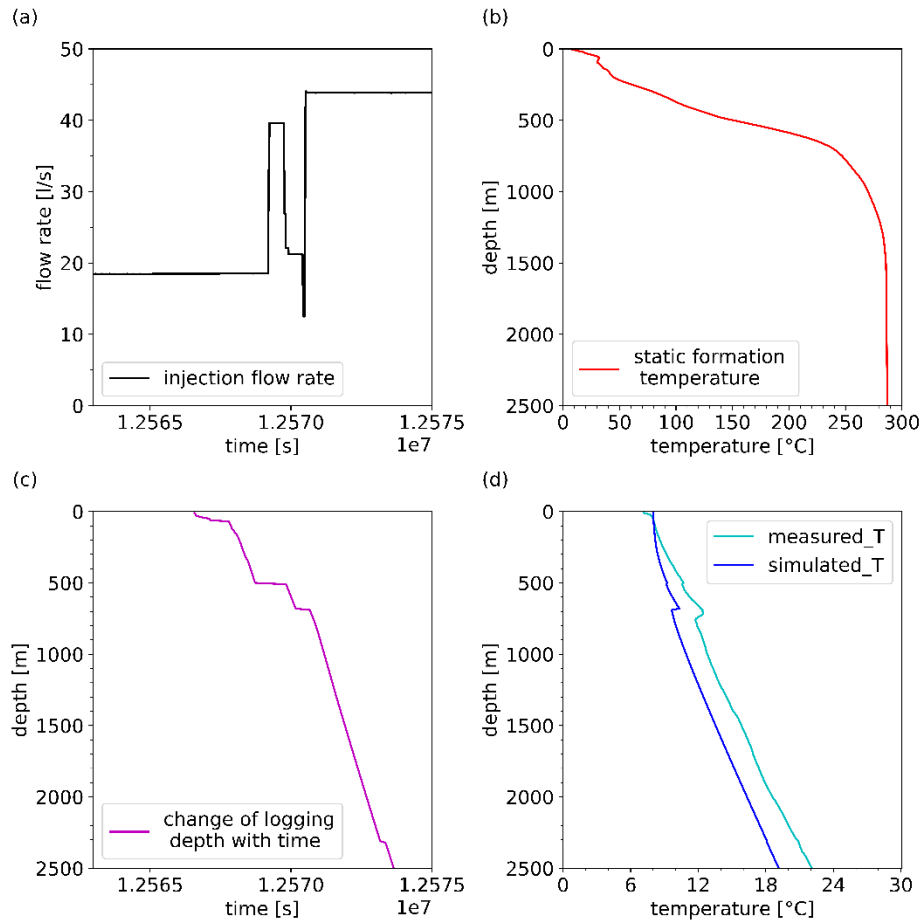


**Figure 7: (a) shows the variation with time of the injection flow rate before, during and after the logging (the x-axis is the time in seconds since the start of the deepening of the RN-15 well). (b) is the static formation temperature profile around the RN-15/IDDP-2 well until 2.5 km (taken from the database). (c) is the change of the logging depth with time, the tripping time of the logging tool from the wellhead to 2.5 km depth is 2 hours. (d) shows the comparison between the simulated temperatures of the well fluid and the measurements at different depths.**

#### 4. CONCLUSIONS AND DISCUSSIONS

Temperature logging data provides important information for the assessment of geothermal reservoirs. However, under specific conditions of high-temperature boreholes, these data may represent a response to various factors such as reservoir temperatures, flow rates, and fluid losses. In this study, the impacts of an individual factor were investigated by a sensitivity analysis using synthetic models. The major conclusions are as follows:

- (1) Applying a simple borehole temperature correction method on the temperature logs obtained under borehole cooling conditions to estimate SFT could lead to huge estimation errors, even when the cooling flow rate is low.
- (2) The local gradient change is affected both by the percentage of fluid loss and the flow rate. For fluid losses < 30% or relatively high flow rates at 20-50 L/s (velocities 0.5~1.3 m/s), the gradient change is independent of the flow rate.

With these findings, the synthetic model approach represents an important step towards a more sophisticated interpretation of real project data where the key factors mentioned above should be taken into account in a combined manner. Work is underway to use dynamic temperature logs for estimating the SFT around the RN-15/IDDP-2 well using inverse modeling techniques. Our primary simulation results for the dynamic temperature logs indicate that the SFT profile from the database provided by ISOR might be underestimated. Moreover, the accuracy of the temperature profile in the shallower 500 m depth is crucial for obtaining a good match between the simulated well fluid temperatures and the logged ones. However, the relatively small differences (< 3°C) between the simulation results and the measurements show that this SFT profile can still be a good initial guess for the SFT estimation.

#### ACKNOWLEDGMENTS

The study is part of the DEEPEGS “Deployment of Deep Enhanced Geothermal Systems for Sustainable Energy Business” Project within European Union’s Horizon 2020 research and innovation program. The support from both the Helmholtz portfolio project “Geoenergy” and the program “Renewable Energies”, under the topic “Geothermal Energy Systems”, is also gratefully acknowledged. We also thank the EnBW Energie Baden-Württemberg AG for supporting geothermal research at KIT. Special thanks to the project coordinator HS ORKA as well as ISOR for providing data gained during the operations at RN-15/IDDP2.

## REFERENCES

- Ascencio, F., García, A., Rivera, J., & Arellano, V. (1994). Estimation of undisturbed formation temperatures under spherical-radial heat flow conditions. *Geothermics*, 23(4), 317-326.
- Ascencio, F., Samaniego, F., & Rivera, J. (2006). Application of a spherical-radial heat transfer model to calculate geothermal gradients from measurements in deep boreholes. *Geothermics*, 35(1), 70-78.
- Bullard, E. C. (1947). The time necessary for a bore hole to attain temperature equilibrium. *Geophysical Journal International*, 5, 127-130.
- Deming, D. (1989). Application of bottom-hole temperature corrections in geothermal studies. *Geothermics*, 18(5-6), 775-786.
- Dowdle, W., & Cobb, W. (1975). Static formation temperature from well logs—an empirical method. *Journal of Petroleum Technology*, 27(11), 1,326-321,330.
- Eppelbaum, L., & Kutasov, I. (2011). Estimation of the effect of thermal convection and casing on the temperature regime of boreholes: a review. *Journal of Geophysics and Engineering*, 8(1), R1-R10.
- Friðleifsson, G. Ó., Elders, W. A., Zierenberg, R. A., Stefánsson, A., Fowler, A. P., Weisenberger, T. B., . . . Mesfin, K. G. (2017). The Iceland Deep Drilling Project 4.5 km deep well, IDDP-2, in the seawater-recharged Reykjanes geothermal field in SW Iceland has successfully reached its supercritical target. *Scientific Drilling*, 23, 1-12.
- Gaston, D., Newman, C., Hansen, G., & Lebrun-Grandie, D. (2009). MOOSE: A parallel computational framework for coupled systems of nonlinear equations. *Nuclear Engineering and Design*, 239(10), 1768-1778.
- Goutorbe, B., Lucazeau, F., & Bonneville, A. (2007). Comparison of several BHT correction methods: a case study on an Australian data set. *Geophysical Journal International*, 170(2), 913-922.
- Hasan, A., & Kabir, C. (1994). Static reservoir temperature determination from transient data after mud circulation. *SPE Drilling and Completion (Society of Petroleum Engineers);(United States)*, 9(1).
- Klepikova, M. V., Le Borgne, T., Bour, O., & Davy, P. (2011). A methodology for using borehole temperature-depth profiles under ambient, single and cross-borehole pumping conditions to estimate fracture hydraulic properties. *Journal of Hydrology*, 407(1-4), 145-152.
- Kutasov, I., & Eppelbaum, L. (2005). Determination of formation temperature from bottom-hole temperature logs—a generalized Horner method. *Journal of Geophysics and Engineering*, 2(2), 90-96.
- Nian, Y.-L., Cheng, W.-L., Han, B.-B., Li, Y.-Q., & Yu, W.-J. (2015). A novel method for predicting gas/oil flow rate from temperature log data. *Journal of Petroleum Science and Engineering*, 133, 801-809.
- Pehme, P., Parker, B., Cherry, J., & Greenhouse, J. (2010). Improved resolution of ambient flow through fractured rock with temperature logs. *Groundwater*, 48(2), 191-205.
- Verma, S. P., Andaverde, J., & Santoyo, E. (2006a). Application of the error propagation theory in estimates of static formation temperatures in geothermal and petroleum boreholes. *Energy Conversion and Management*, 47(20), 3659-3671.
- Verma, S. P., Andaverde, J., & Santoyo, E. (2006b). Statistical evaluation of methods for the calculation of static formation temperatures in geothermal and oil wells using an extension of the error propagation theory. *Journal of Geochemical Exploration*, 89(1-3), 398-404.
- Wong-Loya, J., Andaverde, J., & Santoyo, E. (2012). A new practical method for the determination of static formation temperatures in geothermal and petroleum wells using a numerical method based on rational polynomial functions. *Journal of Geophysics and Engineering*, 9(6), 711-728.